

PFC/RR-92-7

**Technical Appendix to D. Albagli, et al.
Journal of Fusion Energy (1990)**

Calorimetry Error Analysis

S. C. Luckhardt
Plasma Fusion Center
Massachusetts Institute of Technology
Cambridge, Massachusetts 02139

May 1992

In this appendix we will discuss techniques for error analysis in electrochemical calorimetry. The thermal power balance of our calorimeter will be examined, the various heat loss processes and power sources involved in the power balance will be enumerated, the magnitude of possible systematic errors in the power balance will be estimated, and error limits on the measurement of any anomalous heating effects will be discussed. In order to prove the existence of an anomalous heat source, "excess power", we must first show that known variations in heat sources and heat loss mechanisms are not responsible for any observed variations in the calorimeter signal. That is, we must investigate the sources and magnitudes of systematic errors in the power balance measurement. For a discussion of the concept of systematic error and the precision of a measurement see Ref. 1 chapter 6.

The existence of many sources of systematic errors in electrochemical calorimetry, as outlined in this appendix and in Ref. 3, causes us to view with deep skepticism any claims of "excess" heat generation in such experiments. This is one of the main results of our analysis of electrochemical calorimetry, and one of the principal conclusions in Ref. 3. Further, when the known sources of systematic and statistical error are removed from the data set by an analysis procedure outlined in Ref. 3 and explained in further detail in this appendix, we do not find any evidence of an anomalous heating effect in our experiment.

In the following we will show that there are several heat transport processes that can easily give rise to systematic errors in the range of 40-100mW, ~3-6% of the total power input. Thus one cannot validly conclude that "excess power" of this magnitude (or less) was present in our experiment. The physical processes involved in the heat balance of the electrochemical calorimeter are manifold and often difficult to quantify: in the following analysis we derive a ten term power balance equation for the calorimeter. We conclude that accurate calorimetric power measurements over long time periods would require continuous measurement of many distinct heat transport processes.

Our data analysis procedure therefore consists of three steps: first we examine heat transport processes and evaluate their contributions to systematic uncertainties in the measurement of any anomalous heat production, second we examine the calorimetry data and remove drifts and fluctuations caused by known processes, third we compare the remaining fluctuations in the calorimetry data with the ~79mW excess power level claimed in Ref. 2 for 1mm diameter cathodes. As will be shown below, the power fluctuations and drifts that

occurred were explainable by known thermal transport processes causing time dependent fluctuations in the calorimeter power balance. These results do not confirm the level of excess power claimed in Ref. 2, nor any other experimentally significant level of excess power.

CALORIMETER POWER BALANCE

Our experiments were designed to reproduce the experimental conditions and error sources of the experiments reported in Ref. 2. For this reason the electrochemical cell and calorimeter were constructed in a manner similar to that used in Ref. 2 with two principal exceptions: (1) the cell temperature in our experiments was held constant by the addition of a thermostat controlled resistive heating element, (2) The space between the cell and the water bath was filled with glass wool insulator instead of a vacuum space (Dewar cell). The constant temperature method simplifies the analysis of the thermal power balance by eliminating terms involving the time variation of temperature. The glass wool provides a conductive heat flow path and largely eliminates convective and radiative heat flow in the space between the cell and the water bath. The use of thermal conduction heat flow instead of radiative or convective heat flow in the calorimeter simplifies the theoretical analysis of the thermal conductance and reduces systematic errors.

The calorimeter was designed to maintain a steady state heat flow between the cell and the outside environment. Further, thermal gradients in the electrolyte solution will be neglected, it is assumed that constant fluid mixing caused by the passage of electrolysis gas bubbles will eliminate thermal gradients in the fluid. In this situation, the power balance equation can be written as

$$P_{\text{INPUT}} + P_{\text{GEN}} = P_{\text{OUTPUT}} \quad (1)$$

where P_{INPUT} is the total power externally supplied to the calorimeter, P_{GEN} is the sum of all power sources that are internal to the calorimeter, and P_{OUTPUT} is the sum of all power losses from the calorimeter. That is, under steady state conditions, power balance of the calorimeter requires that the total output power from the calorimeter (thermal conduction power, chemical reaction product's potential energy, and all other energy outputs) is equal to the sum of the total power input (electrical energy input to cell, power to internal heating element (P_h) and all other energy inputs) and the power that is generated inside the calorimeter (heat generation caused by any internal processes including anomalous power "excess heat", P_x). As explained in Ref. 3 changes in the cell power balance are detected by changes in the power supplied to the cell from a

thermostat controlled resistive heating element. In the notation of Ref. 3, a time dependent heat source in the cell which generates a power $P_x(t)$, (e.g. excess heat) will manifest itself as a decrease in the cell heater power, $P_h(t)$. Separating out the terms P_x and P_h from the total power balance, Eq. 1 can be rewritten as

$$P_x(t) + P_h(t) = P_o \quad (2)$$

where P_o represents the sum of all the other terms in the calorimeter power balance including input powers and power losses. We call P_o the calibration constant of the calorimeter. Of course, thermal power inputs and losses will not be constant over the duration of the experiment and in general, P_o will be a function of time, $P_o = P_o(t)$. Therefore, observed variations in P_h may be caused by changes in P_o leading to systematic errors in the measurement of $P_x(t)$. To investigate the magnitude of such errors we will first identify the various physical processes involved in the calorimeter heat balance.

The power loss processes contributing to the total P_{OUTPUT} include all thermal transport processes that carry heat from the cell to the outside of the calorimeter. There are six categories of energy transport that must be examined: 1) thermal conduction, 2) thermal convection, 3) radiative heat loss, 4) mass transport 5) evaporative cooling, 6) loss of chemical reaction products. The equation for the output power can be written as:

$$P_{OUTPUT} = \sum_{i=1}^N P_i^{cond.} + \sum_{i=1}^N P_i^{chem.} + P_{EVAPORATION} + P_{RADIATION} + P_{CONVECTION} + P_{MASS FLOW} \quad (3)$$

Where $\sum_{i=1}^N P_i^{cond.}$ is a sum over all thermal conduction paths from the cell to the

outside environment. $\sum_{i=1}^N P_i^{chem.}$ represents the sum of chemical potentials of

all reaction products leaving the cell, for example, the power lost through electrolytic decomposition of D_2O is $P^{chem} \sim 1.5V I_{cell}$. (Recombination effects will be included in the term P^{GEN} in the power balance Eq. 1). If other reactions are present they can be included in this term. The evaporative cooling power P_{EVAP} term arises from continuous evaporation of water from the fluid reservoir and condensation at the top of the calorimeter. The condensation forms water

droplets which fall back into the cell. In this process the latent heat of vaporization of this water is removed from the cell. $P_{\text{RADIATION}}$ represents net power lost from the cell by thermal or black-body radiation processes. This term is small for our calorimeter. $P_{\text{CONVECTION}}$ represents power loss through thermal convection of the saturated air in the cell head space. $P_{\text{MASS FLOW}}$ represents heat carried out of the system by heated water vapor, air, and chemical reaction products which leave the calorimeter through the exhaust tube at the top of the cell, Fig. 2, Ref. 3.

The first term in Eq. 1 can be expanded as

$$P_{\text{INPUT}} = I_{\text{cell}} V_{\text{cell}} + I_h V_h + \sum_{i=1}^N P_i^{\text{ext.}} \quad (4)$$

were I_{cell} , V_{cell} are the measured cell current and voltage, I_h , V_h are the measured heater current and voltage, and the sum is over all other power input processes such as: power from artificial light or sunlight striking the cell, power dissipated by thermal sensors, high frequency oscillations and radio frequency power from the cell power supplies or other electronic equipment, and any other unmonitored sources of power input. These power sources are all probably present at some level in our experiment.

The final term in the power balance equation, Eq. 1 is P_{GEN} which represents power generated inside the cell including the effects of any exothermic (or endothermic) chemical reactions such as recombination of D_2 and O_2 gas, side reactions, state changes in the cathode, other such effects, as well as any anomalous power generated in the cell, $P_x(t)$.

Next we will discuss possible systematic variations in the above power balance processes that can lead to changes in the calorimeter calibration constant $P_o(t)$.

SOURCES OF SYSTEMATIC ERROR IN THE CALORIMETER CONSTANT P_o

THERMAL CONDUCTION PROCESSES

The theory of thermal conduction heat transport in solids is well developed, see Ref. 4 for example. Under conditions of constant temperature the conductive heat transport is described by the Fourier heat conduction law:

$$\Gamma = -\kappa \nabla T \quad (5)$$

and in the one dimensional form, the Fourier law integrated over the conductor gives

$$p_{\text{cond.}} = \frac{\kappa A}{L} [T_{\text{cell}} - T_{\text{ext.}}] \quad (6)$$

where κ is the thermal conductivity of the medium, A is the effective cross sectional area for heat transfer, L is the effective thermal path length between the cell and the outside environment, T_{cell} is the cell temperature, $T_{\text{ext.}}$ is the outside temperature. The thermal conductance of a particular heat flow path, C , is defined as $C = P_{\text{cond.}} / [T_{\text{cell}} - T_{\text{ext.}}]$. For example, the radial heat flow through the glass wool can be modeled as thermal conduction through a cylinder of outer radius $r_b = 3.8\text{cm}$, inner radius $r_a = 1.25\text{cm}$, and height $h = 15\text{cm}$ and from Ref. 5, the conductance C is given by

$$C = \frac{2\pi\kappa h}{\log(r_b/r_a)} = 34\text{mW/}^\circ\text{C} \quad (7)$$

where we have used $\kappa = 0.04 \text{ Wm}^{-1} \text{ }^\circ\text{C}^{-1}$ for glass wool from Ref. 6. Taking the temperature difference between the cell fluid and the water bath as $\Delta T = 20^\circ\text{C}$ we find the power conducted to be $P = 680\text{mW}$. Of course, additional power is conducted through the bottom of the calorimeter further increasing the total. We believe this thermal conduction process is relatively stable over the long term because the glass wool was in a sealed container.

The dominant conduction paths in our calorimeter are: $P_1^{\text{cond.}}$ = conduction through the glass wool insulator to the water bath, $P_2^{\text{cond.}}$ = conduction through the glass body of the cell to the top of the calorimeter, $P_3^{\text{cond.}}$ = conduction through the leads and thermal probes to the top of the calorimeter, $P_4^{\text{cond.}}$ = conduction through the glass wool to the top of the calorimeter. $P_1^{\text{cond.}}$ is the dominant thermal conduction power, but $P_{2,3,4}$ are significant because they produce a steady drift in the conduction power when fluid is lost from the cell, as discussed below.

Next we consider thermal conduction to the top of the calorimeter. This term in the power balance will vary during the course of the experiment because of variations in the amount of fluid in the cell and variations in the temperature of the top of the calorimeter. Variations in the amount of liquid in the cell will cause the distance from the top of the cell fluid reservoir to the top of the calorimeter to vary. This amounts to varying the thermal conduction path length L in Eq. 6, i.e. $L = L(t)$. Denoting the distance from the top of the fluid reservoir to the top of the calorimeter at some particular time $t = t_0$ as $L(t = t_0) = L_0$, we can write $L(t)$ as

$$L(t) = L_0 + x(t) \quad (8)$$

where $x(t)$ describes the subsequent time variation of L .

The variation of the thermal conduction power to the top of the calorimeter then is proportional to $[L_0 + x(t)]^{-1}$. Variations in x are caused by five main processes:

- (1) Electrolytic decomposition of the D_2O causes x to increase.
- (2) Evaporation and exhaust of water vapor from the cell causes x to increase.
- (3) Trapping and release of gas bubbles in the cell can cause x to increase or decrease.
- (4) Condensation of water at the top of the calorimeter causes the formation of water droplets which fall back into the fluid reservoir of the cell, this process causes fluctuations in x .
- (5) Intentional addition or removal of liquid to/from the cell.

These processes will cause systematic changes in P^{cond} , and hence in the calibration constant P_0 . To obtain quantitative estimates of these effects we write the variation of the thermal conductance in terms of the incremental mass added or lost from the cell. Denoting $m(t)$ as the mass of fluid in the cell reservoir at the time t , we have that

$$x(t) = -\frac{1}{\rho A_s} [m(t) - m(t_0)] = -\delta m(t)/\rho A_s \quad (9)$$

where ρ is the density of the fluid, A_s is the fluid reservoir cross sectional area, and $\delta m(t) = m(t) - m(t_0)$. The conductive power to the top of the calorimeter can be written as

$$P^{cond}(t) = \kappa A \frac{(T_{cell} - T_{top})}{(L_0 + x(t))} \quad (10)$$

or in the limit $x \ll L_0$

$$P^{cond}(t) = \kappa A (T_{cell} - T_{top}) \left(1 - \frac{x}{L_0} + \frac{x^2}{L_0^2} + \dots \right)$$

$$\cong \kappa A (T_{\text{cell}} - T_{\text{top}}) \left(1 + \frac{\delta m(t)}{\rho A_s L_0}\right) \quad (11)$$

We can use this equation to calculate variations in P^{cond} caused by $\delta m(t)$.

CALORIMETER BASELINE DRIFT

Eq. 10 predicts that electrolytic decomposition of the D_2O in the cell will lead to a continuous decrease in heater power, P_h in Eq. 2. This is sometimes referred to as a baseline drift of the calorimeter. As is clear from Eq. 10, a decrease in the amount of fluid in the cell will cause $x(t)$ to increase causing a reduction in the thermal conductance to the top of the calorimeter. This leads to a slow decrease of the calorimeter calibration constant P_o in Eq. 2, i.e. loss of liquid ($x > 0$, $\delta m < 0$) mimics excess power. If the rate of electrolytic decomposition and other solvent loss processes are constant and if the cross sectional area of the cell is independent of x , $x(t)$ will increase in proportion to t . Further, if $x/L_0 \ll 1$ is a valid approximation, P_o becomes a linear function of time, i.e. $P_o = a + bt$, with a and b constants.

Long term drifts in the calorimeter baseline can be removed from the calorimeter data by means of linear regression analysis, as will be discussed below. We also note that for sufficiently long duration experiments the x^2 term in Eq. 11 becomes significant causing an apparent lessening in the downward drift of the heater power. Thus in the course of a long duration experiment a continuous loss of liquid from the cell will cause the heater power signal to initially decrease linearly with time, but after a sufficiently long period the rate of decrease in P_h will lessen. In this situation the calorimeter calibration constant P_o will manifest a non-linear variation with respect to t , hence care must be taken in the interpretation of such long time scale variations in P_h .

SYSTEMATIC ERRORS CAUSED BY TEMPERATURE VARIATIONS

Another contribution to systematic variations in thermal conduction to the top of the cell are variations in the temperature of the top of the calorimeter, T_{top} . Since the calorimeter was partially submerged in the temperature controlled water bath, the top of the calorimeter is exposed to room temperature air and in general T_{top} can be different from T_{bath} . Daily changes in room air temperature, heated air from the room heating system, and other similar processes can cause fluctuations in the difference

$$\delta T = T_{\text{top}}(t) - T_{\text{bath}} \quad (12)$$

We can rewrite the temperature difference occurring in Eq. 11 in terms of δT and T_{bath} as

$$P_{\text{cond top}}(t) = \frac{\kappa A}{L_0} (T_{\text{cell}} - T_{\text{bath}}) \left[1 + \frac{\delta m(t)}{\rho A_s L_0} - \frac{\delta T}{(T_{\text{cell}} - T_{\text{bath}})} \right] \quad (13)$$

where for convenience we have neglected terms of order $\delta T \delta m$. This equation allows us to calculate fluctuations in the calorimeter power balance caused by systematic changes in δm and δT once we evaluate the multiplicative thermal conductance with $\delta m = \delta T = 0$. The two factors A_s and A refer to the area of the liquid surface in the cell and the effective area of the thermal conductor(s) respectively.

The effective thermal conductance to the top of the cell can be obtained from measurements of the power change induced by adding a measured quantity of solvent Δm to the cell. In particular, when 5 cm^3 of D_2O was added to the cell we observed a decrease of $\sim 150 \text{ mW}$ in the heater power, Ref. 3 Fig. 6. Thus we find with $T_{\text{cell}} - T_{\text{top}} = \sim 20^\circ\text{C}$,

$$\Delta P_{\text{top}} = 1.5 \text{ mW gm}^{-1} \text{ } ^\circ\text{C}^{-1} (T_{\text{cell}} - T_{\text{bath}}) \Delta m \quad (14)$$

SOLVENT LOSS EFFECT

As discussed above mass can be lost from the cell by exhaust of evaporated D_2O from the cell, or electrolytic decomposition of D_2O . Over the course of our experiment we observed condensation of water in the exhaust tube, and while the amount of water was not monitored quantitatively, it is easily possible that 1 to 2 cm^3 of D_2O was lost over the course of the experiment. According to Eq. 14 this would result in a systematic error in the cell power balance of

$$\Delta P_{\text{error}} = -60 \text{ mW} \quad (15)$$

This negative power increment in P_{OUTPUT} could then be mistaken for an increase in P_x of this magnitude. If the evaporative loss occurred at a constant rate, the result would be an increased baseline drift rate.

GAS BUBBLE TRAPPING EFFECT

Another potentially significant systematic error comes from the process of trapping of gas bubbles in the cell. Such bubbles will raise the level of the liquid in the cell leading to an increase in P_{top} . If a trapped bubble is released, for example, when it reaches a critical size, the liquid level will suddenly drop causing P_{top} to decrease. This effect can also be estimated from Eq. 11. For example if 2 cm^3 of trapped gas is released it is equivalent to the addition of 2 cm^3 of D_2O , hence we can use the above calculation to obtain the power increment of ΔP_{top}

$$\Delta P_{error} = \pm 60 \text{ mW} \quad (16)$$

Over the course of a 200 hour experiment systematic errors of this magnitude would lead to an integrated systematic error in the cell energy balance of 43 kilojoules.

TEMPERATURE VARIATIONS

The effect of systematic variations in the temperature of the top of the calorimeter δT can also be estimated using above data on the conductance along with the cross sectional area of the fluid reservoir $A_s \sim 5 \text{ cm}^2$, $L_0 \sim 3 \text{ cm}$ we find

$$\Delta P_{top} = 22 \text{ mW } ^\circ\text{C}^{-1} \delta T \quad (17)$$

We estimate that fluctuations in T_{top} of magnitude $\delta T = \pm 2^\circ\text{C}$ are possible as a result of daily room temperature variations. Thus this effect contributes a potential systematic error of

$$\Delta P_{error} = \pm 44 \text{ mW} \quad (18)$$

EVAPORATION AND CONDENSATION

Another cause of fluctuations in ΔP_{top} is evaporation and condensation of D_2O . Since the cell temperature is elevated 20°C above room temperature D_2O continuously evaporates from the cell and condenses on the inside top of the calorimeter causing droplets to form and rain down on the fluid reservoir in the cell. This effect will cause rapid fluctuations (time scale minutes to hours) in the fluid level, $\delta x(t)$. Thus we expect some level of approximately random

fluctuations in P_{top} and consequently in the calibration constant P_o . We estimate these fluctuations to be approximately

$$\Delta P_{error} = \pm 10-20 \text{ mW} \quad (19)$$

for a cell with a cross sectional area of 5 cm^2 .

As noted earlier, evaporation and condensation processes in the head space of the cell causes an evaporative cooling of the cell. For example, each gram of water which evaporates from the cell fluid reservoir and condenses on the top of the calorimeter will remove its latent heat of vaporization, approximately 2.2 kJ of heat per gram, from the calorimeter. This effect could lead to systematic errors in the power balance if the evaporation rate of the liquid changed as a result of changes in the cell temperature, or any other parameter which affects the evaporation rate. Since the liquid that is condensed on the top of the cell tends to fall back into the cell and be recirculated, this process does not lead to any loss of mass from the cell and is therefore difficult to detect. If, for example, the evaporation rate changed by 0.1 gm/hr the change in evaporative cooling would change by approximately 60 mW which would be a significant systematic error in the power balance. Further, since the vapor pressures of D_2O and H_2O differ, evaporation will cause a systematic difference in the power balance between the D_2O and H_2O cells.

OTHER SOURCES OF SYSTEMATIC ERROR

In the following we discuss several other sources of systematic error which are more difficult to quantify. As discussed above evaporation and condensation of D_2O in the head space of the cell contributes to the cooling of the cell and is represented by the term P^{EVAP} in the power balance equation Eq. 3. The evaporative cooling term could fluctuate over a long term experiment if there were uncontrolled changes in the evaporation and condensation rate. The air space above the cell is expected to support large convective flows caused by natural thermal convection, and by forced convection generated by the flow of hydrogen gas through the air. This convection cooling would lead to an additional term in the power balance dependent on $x(t)$.

As discussed in Ref. 3 recombination of D_2 and O_2 gas can lead to a large systematic error, the maximum error is of magnitude

$$\Delta P_{error} = 0.2 \text{ A} \times 1.5 \text{ V} = 300 \text{ mW} \quad (20)$$

for the conditions of our experiment. To verify that recombination is not occurring, it is necessary to collect the exhaust gas continuously and monitor the rate of exhaust of D_2 and O_2 .

Measurements of the loss rate of solvent alone are not sufficient to determine the loss rate of deuterium and oxygen gas because other loss processes such as solvent evaporation can be significant in the cell mass balance.

DATA ANALYSIS

As discussed above, the heater power, P_h , and the calorimeter calibration constant, P_o , are expected to display a continuous drift as a result of solvent lost from the cell. If solvent is lost from the cell at a steady rate as a result of electrolytic decomposition and evaporation, we can approximate the downward drift of P_o by a linear relationship:

$$P_o = a + bt \quad (21)$$

where a and b are constants and t is the time variable. Indeed, the raw heater power data shown in Fig. 6 of Ref. 3 displays a continuous downward drift. Thus Eq. 21 represents the simplest model for the complex heat transport processes which contribute to variations in the calorimeter constant P_o over the course of the experiment. Systematic errors discussed in the first part of this appendix can be represented by a general time dependent error term $\varepsilon(t)$. Inserting Eq. 21 into the power balance formula, Eq. 2, adding the error term and solving for P_x we have

$$P_x + \varepsilon(t) = a + bt - P_h \quad (22)$$

The left hand side of Eq. 22 is the sum of excess power and all systematic and statistical error sources, the right hand side is difference between the calorimeter baseline drift and the measured heater power. Thus we can obtain the values of $P_x + \varepsilon(t)$ from the measured values of P_h , and from a and b . This equation was used in the analysis of the heater power data.

DETECTION OF P_x AND LINEAR REGRESSION ANALYSIS

One of the characteristics of the signal P_x that was reported by the authors of Ref. 2 was that P_x is zero during an indeterminate initial "loading period" which may last for several days. After this loading period the excess power would "turn on" and have a magnitude of $\sim 79\text{mW}$ for the case of the 1mm diameter cathode and the current density used in our experiments. Thus we would expect the heater power to decrease slowly because of baseline drift, and then decrease rapidly by approximately 79mW . Thus P_h must exhibit a change in decay rate as the excess power P_x is initiated. On the other hand if the time evolution of P_h can be well represented by a linear function then we can conclude that P_x did not "turn on" during the time

interval in question. In the following we will examine the heater power data by fitting the data to a linear function, and then examining the deviation between the linear fit and the heater power data.

LINEAR REGRESSION METHOD

Linear regression is a commonly used technique for analysis of time series data, such as our heater power data. For a discussion of linear regression and least squares fitting see Ref. 1. Briefly, in linear regression analysis we endeavor to fit a time series data set having an approximately linear variation with time with a continuous linear function of time. The data consists of a set of N data points $[y_i]$ taken at times $[t_i]$. The linear function of time can be represented as $f(t) = a + bt$ where a and b are regarded as adjustable parameters to be chosen in such a way that the values of $f(t_i)$ are a best fit to the data points $[y_i]$. The most convenient criterion for fitting the data is to choose a and b so as to minimize the sum of the square differences between y_i and $f(t_i)$:

$$M(a,b) = \sum_{i=1}^N [y_i - f(t_i)]^2 \quad (23)$$

as shown in Ref. 1 the best fit values of a and b which minimize M are given by

$$b = \frac{\sum_{i=1}^N y_i t_i - \frac{1}{N} \left[\sum_{i=1}^N t_i \right] \left[\sum_{i=1}^N y_i \right]}{\sum_{i=1}^N t_i^2 - \frac{1}{N} \left[\sum_{i=1}^N t_i \right]^2} \quad (24)$$

and

$$a = \frac{1}{N} \left[\sum_{i=1}^N y_i - b \sum_{i=1}^N t_i \right] \quad (25)$$

The coefficients a and b obtained from Eq. 24 and 25 minimize the sum of the squares in Eq. 23 and thus represent the best fit values; $f(t) = a + bt$ is then the linear function that best fits the data. In the following section we will apply the least-squares fitting procedure to the heater power data presented in Ref. 3.

HEATER POWER DATA ANALYSIS

In this section we will follow through the analysis of the calorimeter data from Ref. 3. As explained in Ref. 3, the calorimeter used a feedback controlled heating element to maintain a constant temperature in the electrolytic cells. Any production of "excess heat" would show up as a reduction in the heater power level. The heater power level could be accurately measured by monitoring the current and voltage applied to the resistive heating element. The signal of interest is then the heater power ($P_H = I_H \times V_H$). The level of excess heat claimed in Ref. 2 for our conditions is ~79 mW, this excess was claimed to appear after an initial "loading period" of some hours or days. Thus, to reproduce the claimed effect, we would expect the heater power to undergo a change of the claimed magnitude after some days of "loading".

In our experiments, and those of others using the open cell type calorimeters, the heater power undergoes a steady drift caused by the loss of solvent from the cell. This loss is caused mainly by electrolytic decomposition and evaporation. As solvent is lost, the level of solvent in the cell drops, this causes the thermal conduction path from the solvent to the top of the cell to increase, thus reducing the overall thermal conductance of the cell and reducing the rate of heat flow out of the cell. To maintain constant cell temperature, the heater power must also decrease slowly. This base line drift trend can be seen in the raw heater power plots in Fig. 6 of Ref. 3.

To analyze the heater power data we employ the reduced power balance equation, Eq. 22. The values of a and b in Eq. 22 are not known *a priori*, so they must be found by regression analysis of the heater power data. After we remove the baseline drift, then any onset of anomalous heating would appear as an excursion from zero. In particular, in the attached Figs. 1a and 1b we show the raw heater power data P_H for the D_2O cell, and the linear regression fit Y_H to the raw data. The best fit regression coefficients ($Y_H = a + bt$) are $b = -3.6 \text{ mW/Hr}$, $a = 1.55 \text{ Watts}$. In Fig. 2a the difference $P_x + \varepsilon(t) = Y_H - P_H$ is shown. To remove the high frequency fluctuations, the data is time averaged, Fig. 2b. The time averaging was accomplished by using MATLAB signal processing software [Ref. 7]. As discussed above the high frequency fluctuations are believed to be caused by the trapping and escape of gas bubbles from under the Teflon supports for the cell electrodes, (see drawing of the cell in Fig. 2 of Ref. 3) and by condensation in the cell which causes water droplets to occasionally fall

back into the cell. These effects cause fluctuations in the cell fluid level and as explained above result in heater power fluctuations.

Since we are attempting to detect the onset of a sustained change in the cell power balance we are not interested in the rapid fluctuations in the data shown in Fig. 2a. To remove these fluctuations we average the data over one hour time blocks, the result of the averaging is shown in Fig. 2b. The time averaged data has one main feature, a slow variation having a 24 hour period. We note that both the D₂O and H₂O cells exhibit this feature. Evidently these fluctuations are not the sought excess heat effect which was reported to occur only in D₂O cells. We believe this is caused by daily room temperature variations which can contribute a significant systematic error to these measurements as discussed above. The potential magnitudes of these systematic errors can easily be in the 20-40mW range as calculated above. Aside from this 24 hour period variation, the data is quite close to zero with some residual fluctuations in the range of 10-20mW.

From the above analysis of the D₂O calorimeter data, including subtraction of a linear baseline drift, averaging of rapid fluctuations, and removal of systematic errors having a 24 hour period, we find only small fluctuations in the range of 10-20 mW which can be attributed to other systematic error effects as enumerated in the first part of this paper. There does not appear to be any evidence of the onset of the claimed anomalous heating event of magnitude 79mW in Fig. 2. This conclusion was stated in our paper.

As noted in the caption of Fig. 6 in our paper, the data sampling rate for the D₂O cell power was reduced at t=30 hours. This was done to save disk space on the data acquisition computer. The regression analysis described above tends to weight the initial data more heavily because of its higher sampling rate. We can also perform a regression with a uniform data sampling rate by filtering and resampling the data taken for t<30 hours. This effectively reduces the sampling rate by a factor of two yielding a new data set having a uniform sampling rate throughout. These data were then subject to linear regression and baseline subtraction as before. The result of this analysis, shown in Fig. 3 a and b is almost indistinguishable from the results of the original analysis shown in Fig. 2. The time averaging and linear regression was done using MATLAB signal processing software, Ref. 7. Our conclusion from this analysis is the same as before.

The analysis of the H₂O cell data is shown in Figs. 4 and 5. The heater power data is shown in Fig. 4a, the best fit regression line in Fig. 4b. The regression coefficients are $b = -5.6\text{mW/Hr}$, $a = 1.67\text{Watts}$. After the baseline subtraction the quantity $P_x + \varepsilon(t)$ is plotted in Fig. 5a, and the time averaged signal in Fig. 5b. Note the in Fig. 5 there is a residual, 24 hour period

variation in the heater power which is similar to the variations evident in Fig. 2. As discussed above we believe this is an error signal caused by the daily variation of heat transport to the top of the calorimeter.

A comparison of the systematic differences between the heater power data in the two cells can also be done. The general characteristics of the heater power signals from the two cells were quite similar, both exhibited rapid fluctuations, a linear baseline drift, and long time scale oscillations with a 24 hour period. We note that the baseline drift and amplitude of the rapid fluctuations were both somewhat larger in the H₂O cell. This difference in magnitude was a constant feature of the two calorimeters throughout the course of the experiment, and thus cannot be related to the sought anomalous power production which was claimed to manifest itself only after a long "charging period" and only in the D₂O cell. The analysis of systematic error sources provides several possible contributions to the differences the two calorimeters.

The fluctuations and baseline drift predicted by Eq. 13 are dependent on the distance L_0 between the top of the cell fluid and the top of the calorimeter. Thus, any difference in the physical dimensions of the two calorimeters, or the volume of the internal structure of the calorimeter would lead to a systematic difference between the values of L_0 between the two cells. If such a difference in L_0 exists, then as shown by Eq. 13 there will be a systematic difference in the baseline drift and fluctuation level of the two calorimeters. Similarly, differences in the cross sectional areas, A_s , of the fluid reservoirs would also result in differences in the baseline drifts as indicated by Eq. 13.

Thus small differences in the physical dimensions of the calorimeters can cause variations in the baseline drift and fluctuation levels between the two. Other processes also contribute to systematic differences between the two calorimeters including differences in the vapor pressures of D₂O and H₂O which would cause different rates of evaporative cooling and evaporative mass loss in the two. Further, the differences in drift and fluctuation level cannot validly be attributed to excess heat effects since those effects are claimed to occur only after an initial charging period in D₂O cells. The difference of the baseline drift and fluctuation level between the two cells was a constant feature throughout the duration of our experiments and was largest in the H₂O cell, therefore we cannot attribute it to the sought excess heat effect.

FIGURE CAPTIONS

Fig. 1 (a) D₂O cell heater power data. (b) Best fit regression line to data in 1a.

Fig. 2 (a) D₂O cell data after baseline drift subtraction. (b) Time average of data from 2a.

Fig. 3 (a) D₂O data after baseline drift subtraction, linear regression done on data having a constant sampling rate. (b) Time average of data from 3a.

Fig. 4 (a) H₂O cell heater power data. (b) Best fit regression line to data in 4a.

Fig. 5 (a) H₂O cell heater power data after baseline drift subtraction. (b) Time average of data from 5a.

REFERENCES

1. J. Mandel, *The Statistical Analysis of Experimental Data*, Dover Publications, Inc. (1984).
2. M. Fleischmann, S. Pons, and M. Hawkins, *J. Electroanal. Chem.* **261**, 301; **263**, 187 (1989).
3. D. Albagli, et al., *J. of Fusion Energy*, **9**, 133 (1990).
4. H. S. Carslaw and J.C. Jaeger, *Conduction of Heat in Solids*, Oxford University Press (1986).
5. D.R. Pitts and L.E. Sissom, *Theory and Problems of Heat Transfer*, McGraw-Hill, Inc. (1977).
6. R.C. Weast, M.J. Astle, eds, *CRC Handbook of Chemistry and Physics*, CRC Press, Inc. (1979).
7. PC MATLAB, *The Signal Processing Toolbox*, The MathWorks, Inc. (1990). MATLAB is a registered trademark of The MathWorks, Inc.

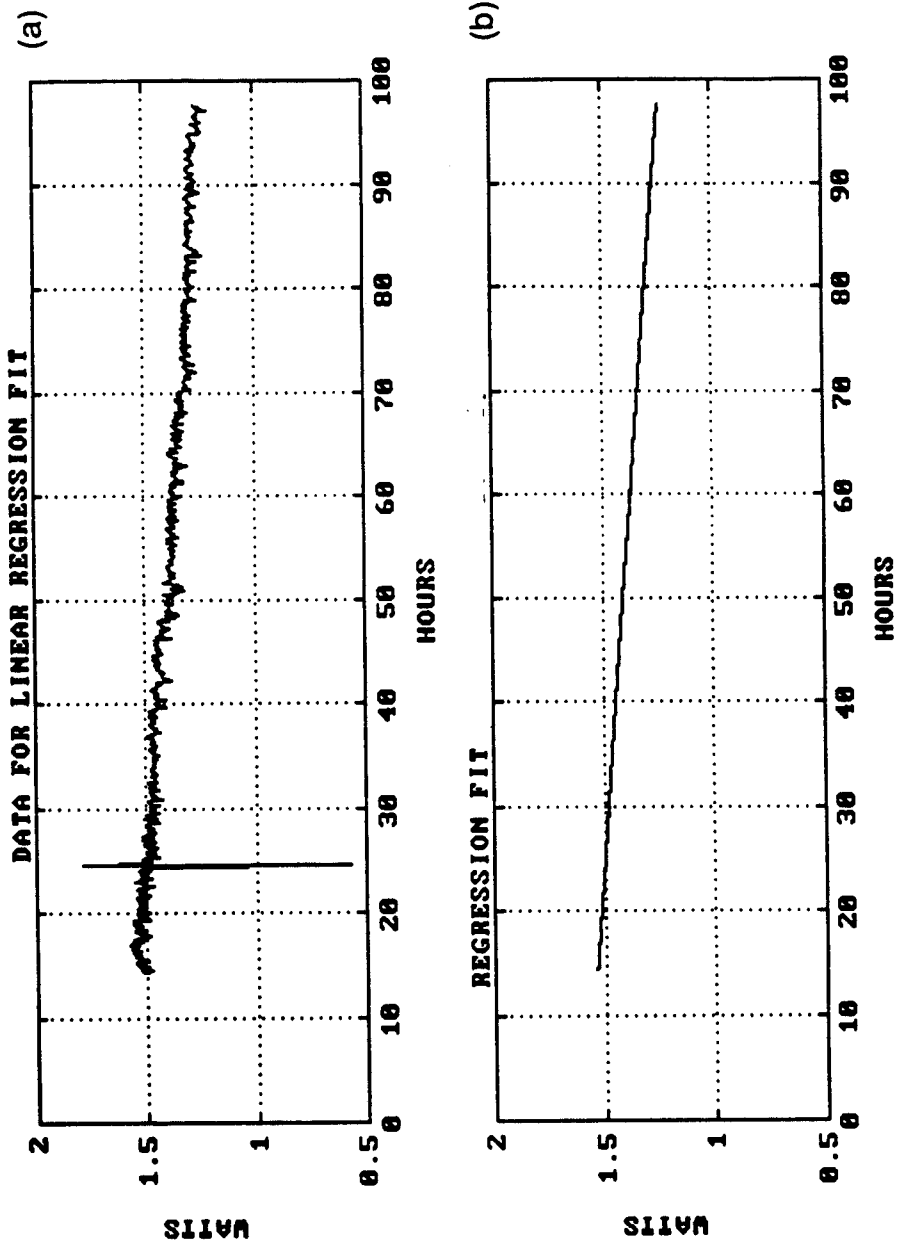


Fig. 1

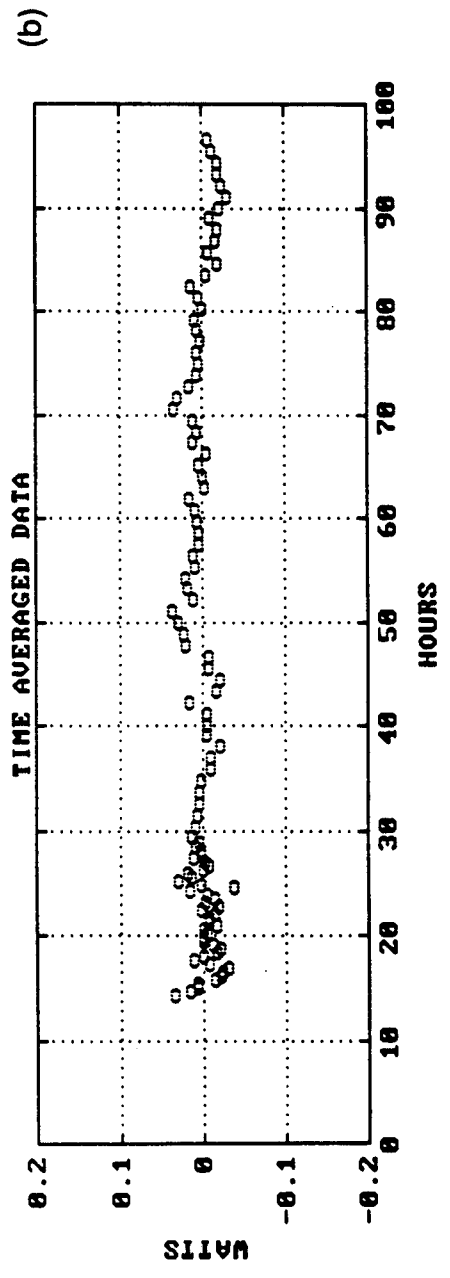
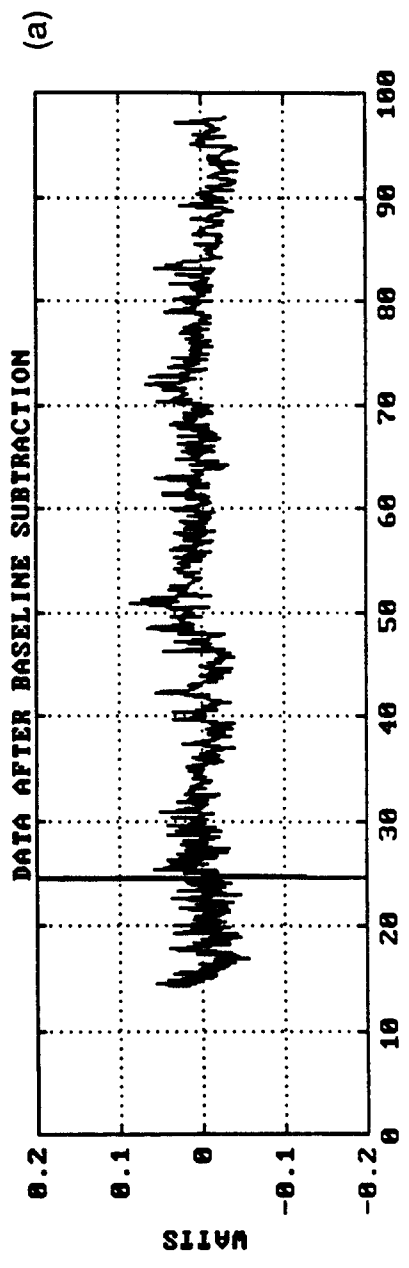


Fig. 2

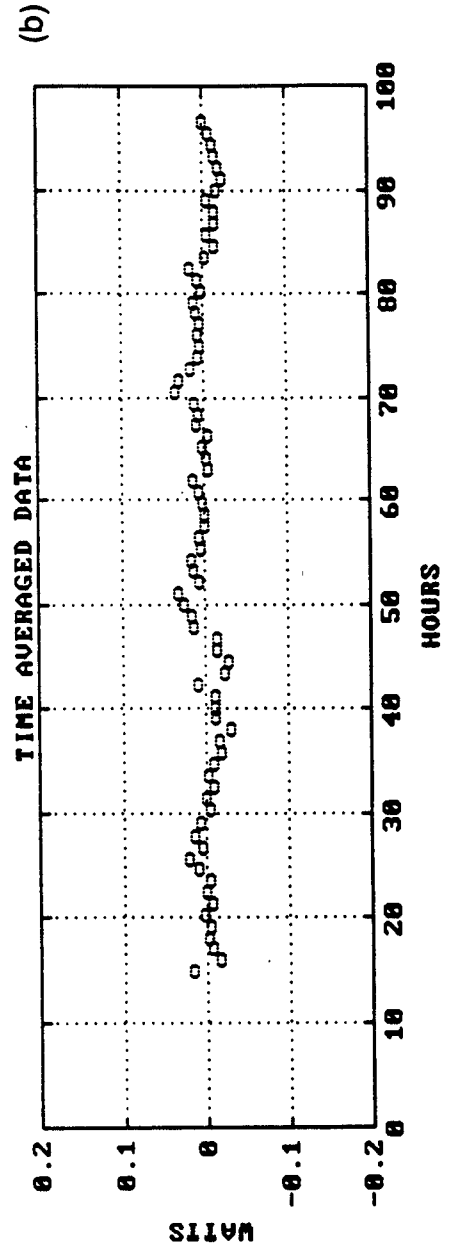
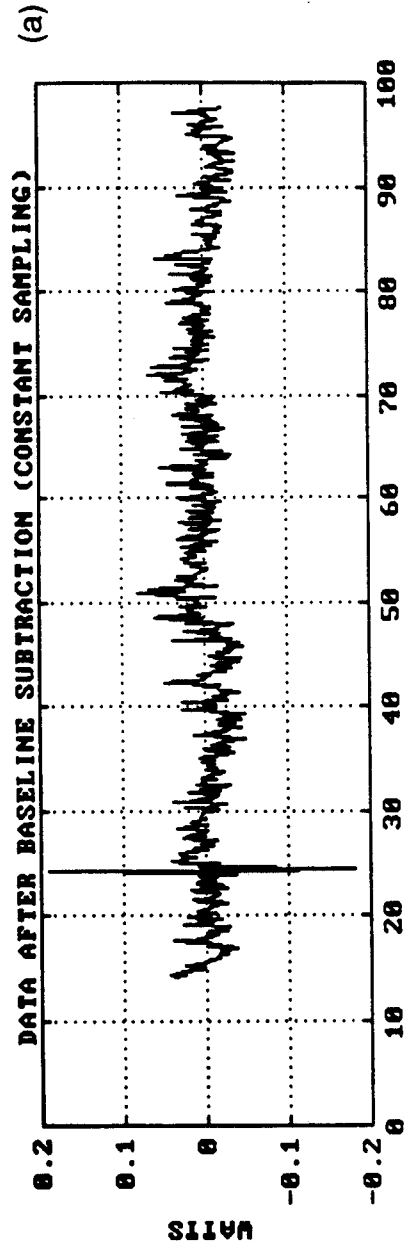


Fig. 3

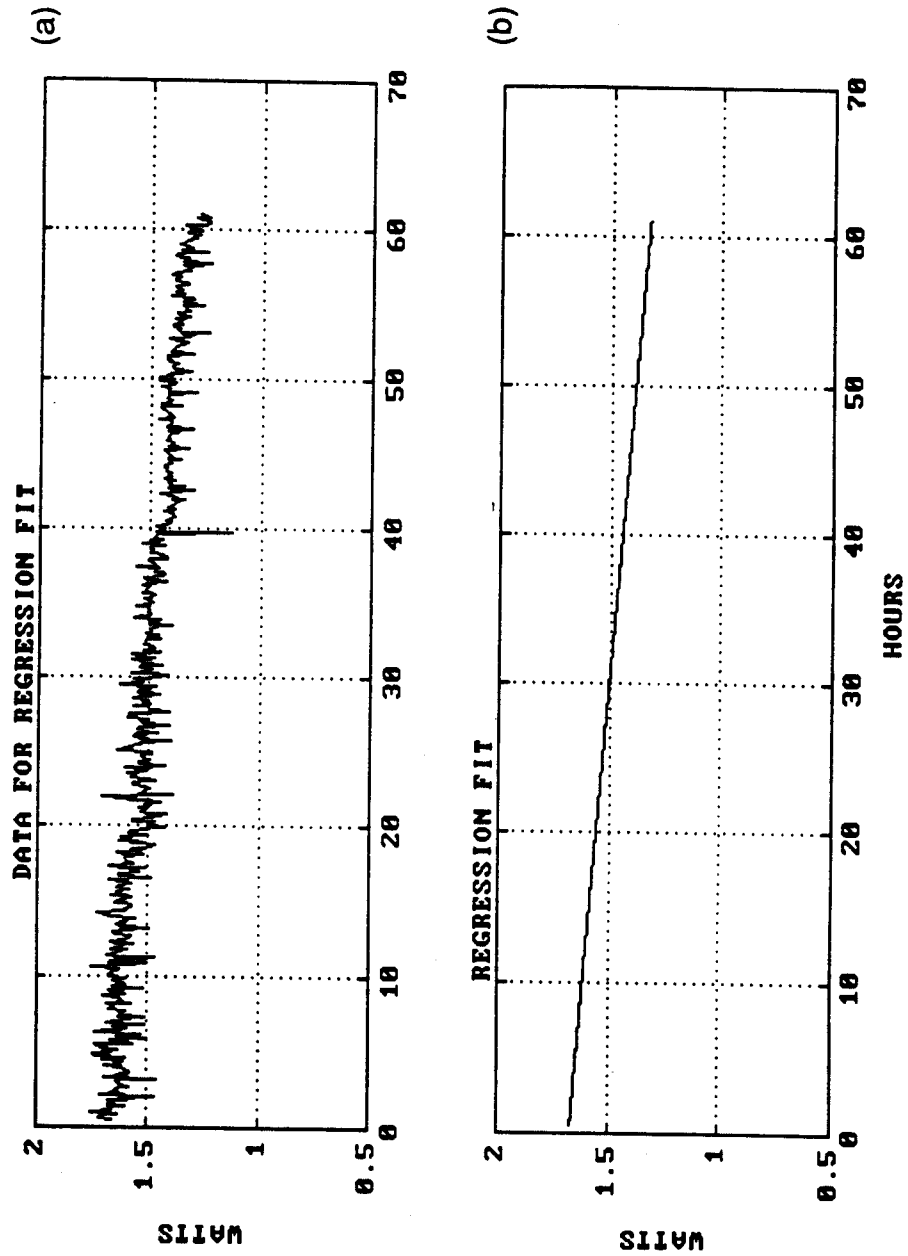


Fig. 4

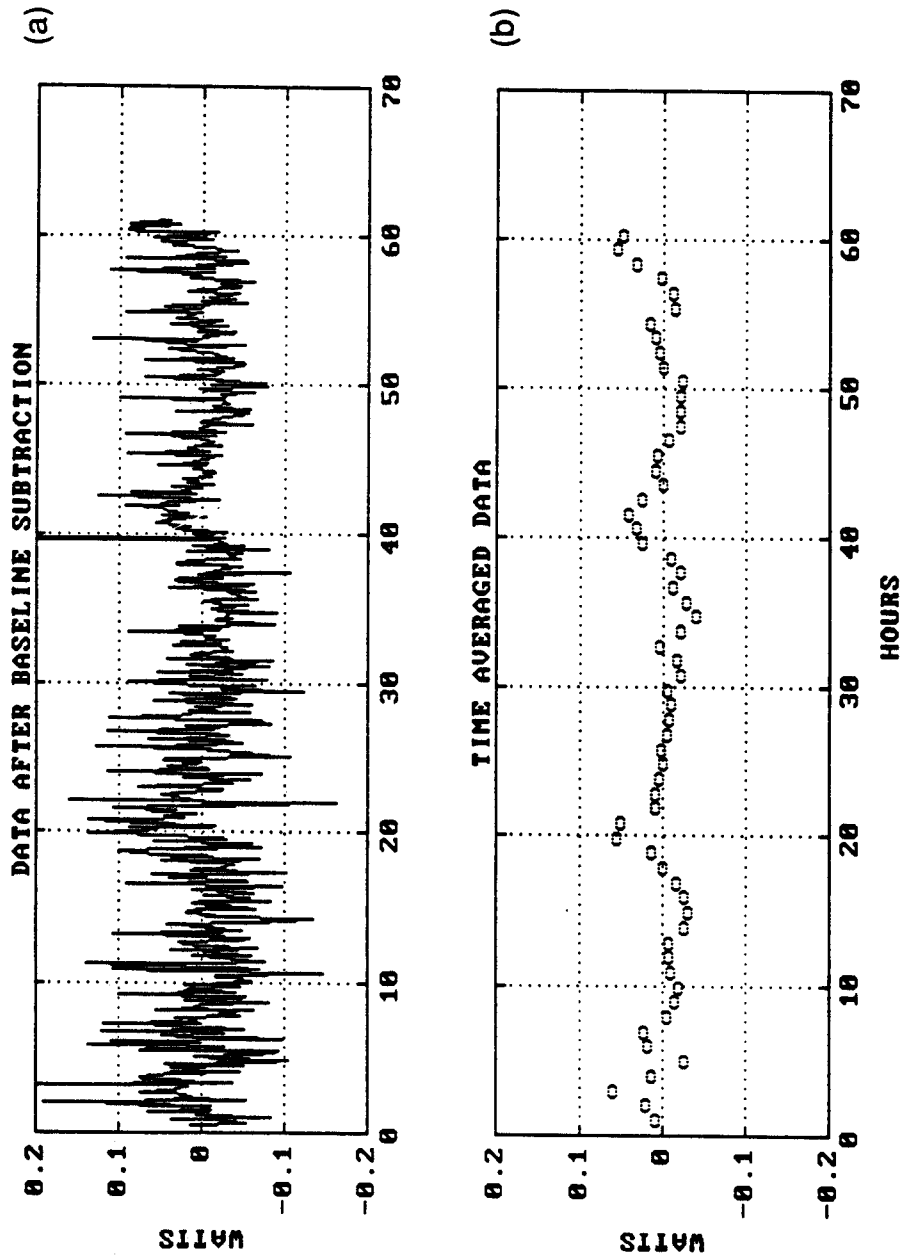


Fig. 5